

This article was downloaded by:

On: 23 January 2011

Access details: *Access Details: Free Access*

Publisher *Taylor & Francis*

Informa Ltd Registered in England and Wales Registered Number: 1072954 Registered office: Mortimer House, 37-41 Mortimer Street, London W1T 3JH, UK



International Journal of Polymeric Materials

Publication details, including instructions for authors and subscription information:

<http://www.informaworld.com/smpp/title~content=t713647664>

Crystallization Under Extreme Temperature and Pressure Gradients

H. D. Noether^a

^a Celanese Research Company, Summit, New Jersey

To cite this Article Noether, H. D.(1979) 'Crystallization Under Extreme Temperature and Pressure Gradients', *International Journal of Polymeric Materials*, 7: 1, 57 – 82

To link to this Article: DOI: 10.1080/00914037908077914

URL: <http://dx.doi.org/10.1080/00914037908077914>

PLEASE SCROLL DOWN FOR ARTICLE

Full terms and conditions of use: <http://www.informaworld.com/terms-and-conditions-of-access.pdf>

This article may be used for research, teaching and private study purposes. Any substantial or systematic reproduction, re-distribution, re-selling, loan or sub-licensing, systematic supply or distribution in any form to anyone is expressly forbidden.

The publisher does not give any warranty express or implied or make any representation that the contents will be complete or accurate or up to date. The accuracy of any instructions, formulae and drug doses should be independently verified with primary sources. The publisher shall not be liable for any loss, actions, claims, proceedings, demand or costs or damages whatsoever or howsoever caused arising directly or indirectly in connection with or arising out of the use of this material.

Crystallization Under Extreme Temperature and Pressure Gradients†

H. D. NOETHER

Celanese Research Company, Summit, New Jersey, 07901

(Received March 20, 1978)

Crystallization under high temperature or pressure gradients is observed in extrusion-orientation processes such as fiber formation during spin-orientation.

Thermodynamic considerations indicate that crystallization temperatures and rates of crystallization in such processes are tremendously increased. For materials crystallizing fast and to a high degree (for example polypropylene), the increased crystallization rates at high spin stresses lead to well oriented lamellar structures which form epitaxially on the originally produced fibrillar nuclei and fibrillar crystallites. For slow crystallizer (such as polyethylene terephthalate) high spin-stress extrusion leads to an oriented, crystalline fibrillar system.

The lamellar structures show highly elastic properties to high extension (50–100%) and over an extensive temperature range (–180 to 140°C for polypropylene) especially after perfecting the lamellar morphology by annealing.

The elastic mechanism of these “hard” elastic materials is elucidated on the basis of X-ray diffraction, electron microscopy, and other studies. A major part of the reversible extension seems to be energy elastic due to the deformation of lamellae and reversible void formation of the interlamellar regions.

This special lamellar morphology is intermediate between the unoriented spherulitic morphology obtained at low extrusion stresses and a largely fibrillar morphology obtainable by subsequent drawing or by extrusion of exceptionally stiff polymers. While the hard elastic materials at present have not found technical applications, a microporous derivative has been commercialized.

The study of crystallization under extreme temperature and pressure gradients basically is concerned with the investigation of crystallization during high speed extrusion processes such as modern fiber spinning and film extrusion operations.^{1,2}

Fiber production methods involve melt, dry or wet (solution) spinning,³ depending on the melt stability or solubility of the fiber-forming polymer and

†Presented at a Symposium on “Flow-Induced Crystallization” at the Midland Macromolecular Institute, August 22–26, 1977, R. L. Miller, Chairman.

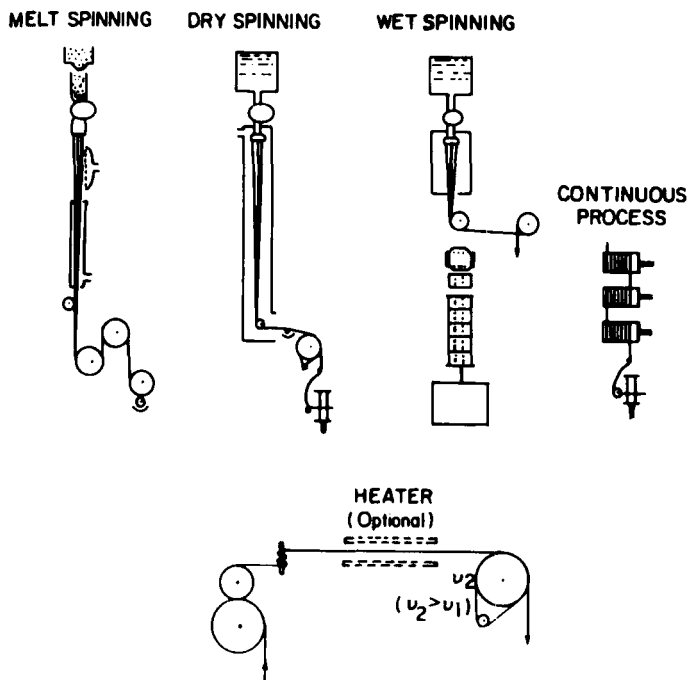
SPINNING

FIGURE 1 Fiber formation and orientation processes.

also the desired tensile characteristics of the products. Figure 1 shows a schematic of these processes.

Normal melt spinning processes involve two steps: (1) the accurately metered extrusion of a polymer melt through a spinnerette of from 1 to 1,000 holes to yield an *unoriented* crystalline or amorphous filament bundle; and (2) the drawing at room or elevated temperatures, in steam or over pins, etc., with draw ratios from 2–10 to yield fibers with the known properties of commercial yarns, staple, tire cord, etc. Any melt-spinnable polymer (e.g. polyethylene, polypropylene, nylons, polyester) was and still is being produced in this manner.

Wet spinning processes, because of the tenderness of the filaments at the spinning jet in their initial state of formation, are quite slow. Precipitation and orientation steps are usually combined and for economic reasons tremendous fiber bundles are extruded at each spinning jet.

Dry-spinning with solvent evaporation during the fiber formation process allows considerably higher extrusion speeds. It also allows production of oriented, finished yarn in one process (as, for example, cellulose acetate or

triacetate) or of an unoriented material to be drawn subsequently similar to yarns produced by melt extrusion (for example polyacrylonitrile).

The economic advantages of high speed extrusion combined with simultaneous orientation of fibers or films are obvious, the finished product is available in larger quantity, faster, with fewer operations and simpler machinery. Up to the present time the scientific investigation of such processes in the published literature has been limited largely to melt extrusion studies. There are few references to extreme pressure gradients in extrusion processes, the major ones being an explosive extrusion of polyethylene from a methylenechloride solution⁴ at 200°C or of PET from methylenechloride to give a foamed material.⁵ The extruded polyethylene could be drawn subsequently to a product of very high modulus (429 g/den) and tensile strength (~20 g/den). Cellulose acetate or triacetate spinning also fits into extrusion under high pressure gradients; extrusion temperature is considerably above the boiling points of polymer solvents.

Thus, the following discussion will have to concern itself primarily with melt extrusion studies and high temperature gradients. Early work of high speed melt extrusion was directed towards Nylon⁶ and polyester. The products yielded desirable strengths and moduli for textile applications, provided high speeds were used and heated tubes were added to the spin line. However, the authors always indicated that the observed elongations at break were considerably higher than desired and certainly higher than those found in the two-step melt spin and "cold draw" process (Figure 2). The fiber structure model of that time was believed to be the fringed micelle. Therefore, it was

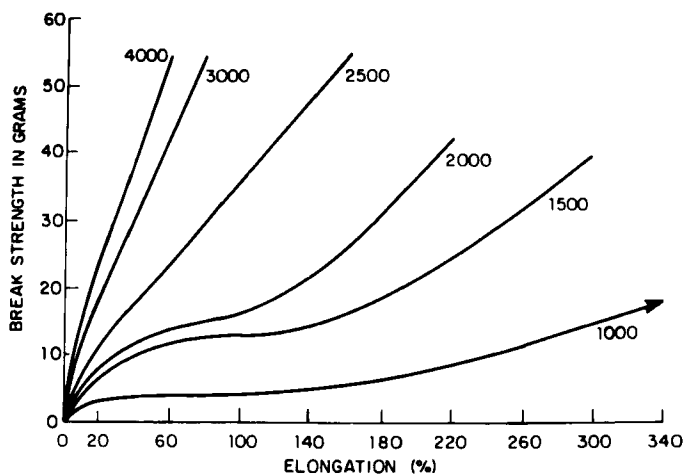


FIGURE 2 Stress-strain curves of spin-oriented Nylon 6 as a function of take-up velocity (in m/min). After Griehl and Versäumer.⁶

difficult to explain the differences in tensile characteristics. Degree of orientation as observed by wide angle X-ray diffraction appeared equivalent for both the spin oriented and the spun and subsequently drawn products.

The differences in superstructure, i.e. the relative concentrations of folded lamellar and fibrillar highly extended chains were unknown at the time. In retrospect, it seems clear that stress-spin orientation produced a superstructure with a higher concentration of oriented folded chains, lamellar units. The high elongations at break would correlate with their partial hard elastic character with fewer load bearing and also less oriented interlamellar connections.

In recent years commercial interest in high speed extrusion processes, development of improved understanding of polymer morphology, and considerable expansion in variety and sophistication of physical tools to observe the physical, morphological, and mechanical characteristics as functions of operating variables, has led to a tremendous increase of research in this field,¹ with a more quantitative understanding of the primary variables responsible for a specific morphology and properties in fibers.

An extensive theory of extrusion processes has been derived,^{3,7} the results of thermodynamic considerations^{8,9} have been verified by experimental studies.

Experimental approaches to the study of high speed processes can be divided into two groups: (1) the normal evaluation of chemical, physical, and mechanical properties of the process products by thermal, thermomechanical, optical, electron, X-ray, and optical diffraction and mechanical methods, correlating these data with the major process variables: polymer molecular weight, spin stress,¹ extrusion temperature, cooling rate; and (2) the much more difficult task of obtaining process data of local filament temperature, filament dimensions, yarn speed, location of the onset of crystallization, and crystallization rate along the spin line.^{2,10,11} Sophisticated instrumentation has been and is being developed to measure yarn diameter, filament speed and temperature, orientation factors, crystallization, and type of morphology. However, some methods, for example X-ray diffraction,² still require relatively long exposures and large filament diameters and thus place limits on this approach. A Japanese group² was probably first in designing an experimental unit, using a specially strong rotating anode X-ray source (to 300 MA) directly built into the spin line to study the extrusion process *in situ* for polyethylene, polypropylene, and poly(butene-1) by small angle (SAXR) and wide angle X-ray (WAXR) diffraction photographic methods, obtaining also orientation data, filament diameter, surface temperatures, and onset of crystallization of a monofilament along the process line. A more recent design by the University of Tennessee¹¹ group is shown in Figure 3.

The research of these two groups has shed considerable light on the effect

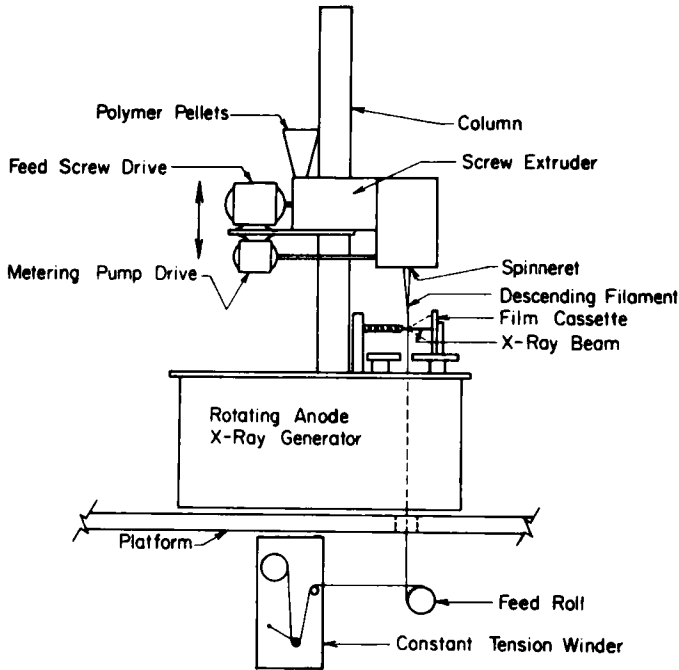


FIGURE 3 Schematic of experimental spinning equipment. From Dees and Spruiell.¹¹ (With permission of John Wiley and Sons, New York.)

which temperature and spin stress have on properties and morphology of the resulting fibers. However, the difficulties of observing the *in situ* changes along the spin line have limited their approach to relatively heavy denier monofilament work. Only very recently, publications of high speed spinning of multifilament yarns are appearing in the open literature (see below: data on polyethylene terephthalate). However, here the analysis covers only the study of the properties of the finished fibers (Approach No. 1). Some data are usually given as to polymer viscosity, extrusion temperature, spin orifice dimensions, take-up speed, through-put and filament diameter or denier. No *in situ* data (Approach No. 2) are reported.

The extent of this work and its broad interest is best demonstrated by the number and range of contributions at the ACS symposia in April and August 1975.^{1,7} Ziabicki's book covers in detail both theory and practice of fiber formation processes including some theory and data on spin orientation studies and gives complete literature references of developments in this field.

The thermodynamics of the stress-spinning processes have been summarized admirably by Peterlin.⁹ The elongation and orientation of randomly coiled macromolecules in the strained melt reduce their entropy. Since this

deformation does not affect the heat content, decrease in entropy increases the equilibrium crystallization or fusion temperature.⁹

At a given temperature T , the super cooling $\Delta T = T_m - T$ is larger for strained oriented polymer chains, than for those relaxed. This reduces the required size of the primary nucleus (proportional to $(1/\Delta T)^3$) and of the secondary nucleus (proportional to $(1/\Delta T)^2$). The rate of crystal growth increases exponentially with $(\Delta T)^2$. Thus, in stress spinning, nucleation and crystallization start earlier and are several hundred times faster than for the unstrained melt.⁹

The *in situ* studies by the Japanese and University of Tennessee groups^{2,11} have experimentally determined the changes in crystallization rates and crystallization temperatures as a function of spin stress. Figure 4 shows schematically continuous cooling transformation (CCT) curves as proposed by Spruiell and White¹⁰ on the basis of spin line data. These curves are used to compare the kinetics of crystallization of melt stress-spinning to those of quiescent melts. Increased stress ($\sigma = K$) places the CCT curve well to the left of the quiescent curve (stress = $\sigma = 0$) on the time scale. The onset of crystallization for stressed and quiescent melts falls on different curves and for the former also depends on the cooling rate; however, the stressed melt crystallization point is always higher than the corresponding value for the quiescent melt. The Tennessee group¹¹ also proposed a model of changes in morphology as function of spin stress (Figure 5).

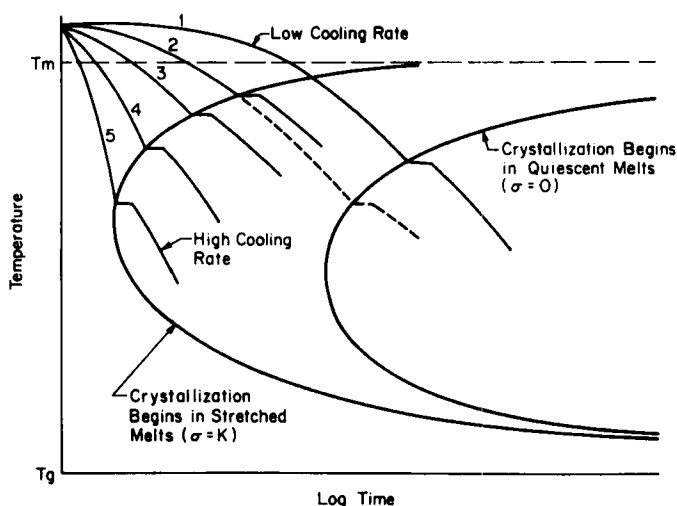


FIGURE 4 Schematic of continuous cooling transformation curves as a function of spin stress. (σ = spin stress, such as O, K.) From Spruiell and White.¹⁰ (With permission of Society of Plastics Engineers, Inc.)

Crystallization During Melt Spinning of Linear Polyethylene

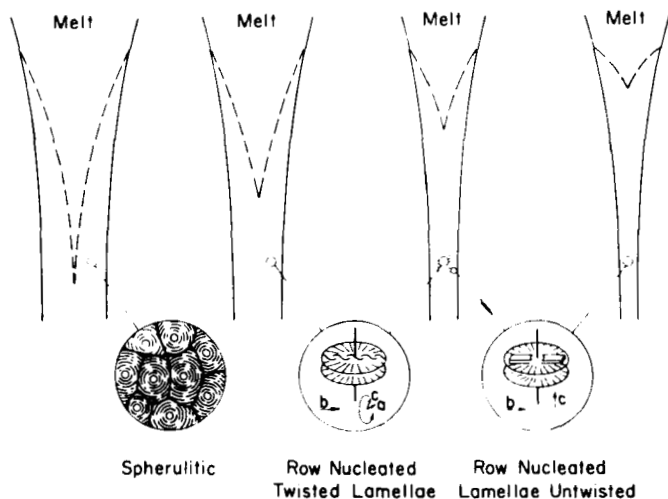


FIGURE 5 Morphological models of structures as a function of spin stress. (Take-up velocity increases from left-to-right.) From Dees and Spruiell.¹¹ (With permission of John Wiley and Sons, New York.)

The crystallization rates of polymers, even in the quiescent state, are vastly different as is the super-cooling required for polymer crystallization to start. Figure 6 presents some of the data compiled by Wunderlich.¹² For example

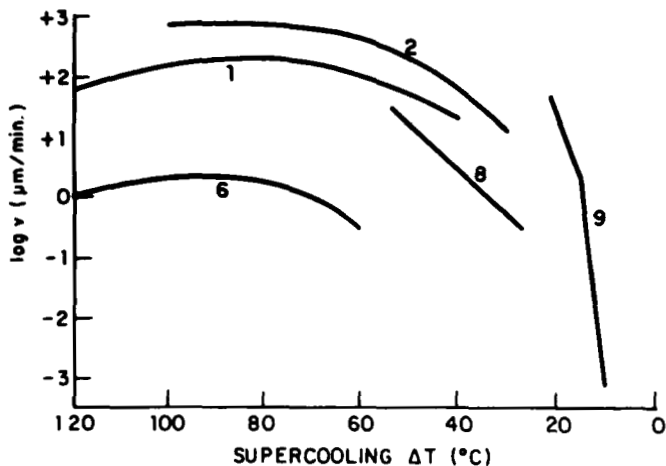


FIGURE 6 Logarithm of crystal growth rates as a function of supercooling: (1), Nylon 6; (2), Nylon 6,6; (6), poly(ethylene terephthalate); (8), polypropylene; (9), polyethylene. After Wunderlich.¹²

poly-(ethyleneterephthalate) (PET) and polypropylene have very different crystallization rates as well as differences in the temperature differential (ΔT) between the melting point and onset of crystallization.

In the following, polypropylene (PP) and poly(ethyleneterephthalate) (PET) will be used to demonstrate the effects of spinning variables on the details of high stress melt extrusion processes.

A major melt spinning study of polypropylene by Sheehan and Cole¹³ evaluated the effect of spin orientation and morphology on the maximum tensile strength obtainable by subsequent drawing. They observed that both crystalline or smectic forms of polypropylene could be obtained in the spinning process as function of quench rate and temperature. Air cooling gives the normal monoclinic structure; water quench (room temperature or below) produces an oriented, smectic structure. Tenacity after drawing was found to increase with molecular weight, higher draw ratio, the smectic material being more readily drawable.

Figure 7 shows the effect of decreasing extrusion temperature and increasing spin stress on the morphology of the resulting "as spun" product.¹⁴ Orientation and crystallinity increase with decrease in extrusion temperature, the morphology changing from a spherulitic to a well oriented, lamellar structure equivalent to the model shown earlier¹¹ (Figure 5). Crystalline orientation factors seem to be independent of extrusion temperature and a function only of the spin line stress.^{1,10,15}

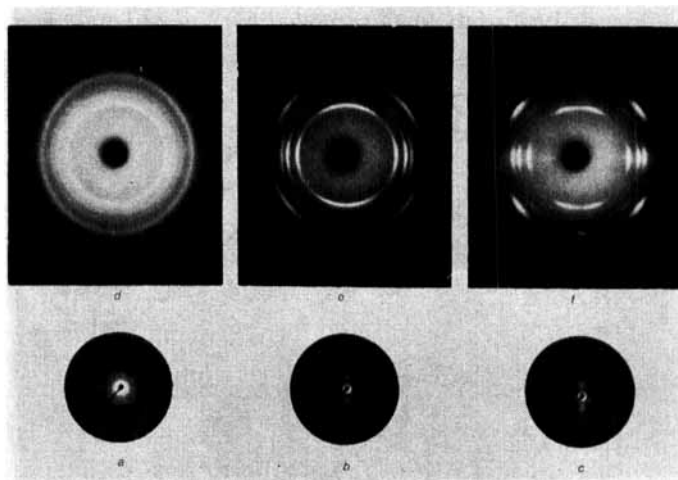


FIGURE 7 Polypropylene samples with different degrees of order and orientation. "As spun" function of extrusion temperature and increasing spin-stress with decreasing extrusion temperature. Top row, WAXR; bottom row, SAXR. a and d, 320°C; b and e, 280°C; c and f, 230°C. From Noether and Whitney.¹⁴ (With permission of Dr. Dietrich Steinkopff Verlag, Darmstadt.)

A unique diffraction pattern, characteristic of the crystalline, oriented, stress spun polypropylene has aroused considerable discussion. A so-called "bimodal" or doubly oriented system is observed—one part showing *c*-axis orientation, with *a* and *b* axes cylindrically arranged around the *c* axis (diffraction spots on the equator), the other with the *a'* axis in the fiber direction and *b* and *c* axes cylindrically arranged around the unique *a'* axis (for details see Ref. 15). A number of explanations have been given.¹⁶ It has been proposed that the original orientation is due to *c*-axis oriented nuclei forming *c*-axis oriented fibrils, followed by epitaxial over-growth of *c*-axis oriented lamellae. The *a'*-axis oriented crystallites follow later. It seems that their dimensions are smaller and they melt at a lower temperature. Clark¹⁶ has proposed a model showing the *a'*-axis oriented crystallites in interlamellar regions (Figure 8). Thermomechanical measurements of Göritz and Müller^{16a} on hard elastic fibers, which have the same morphology as these spin stress oriented fibers, indicate that on extension a thermal effect takes place which they correlate with a small amount of melting in the interlamellar regions. This could very well be due to the *a'*-axis oriented crystallites which Clark¹⁶ locates in these regions. The concentration of these special crystallites as function of

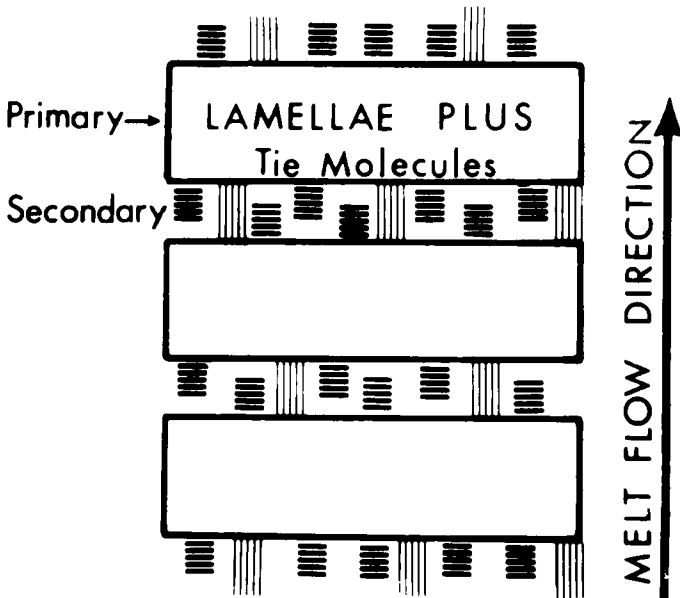


FIGURE 8 Proposed morphology of polypropylene with bimodal orientation, showing primary and secondary crystallization stages. From Clark and Spruiell.¹⁶ (With permission of Society of Plastics Engineers, Inc.)

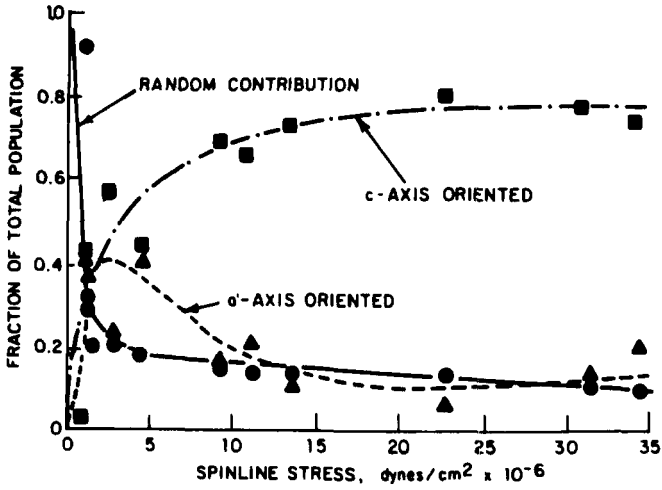


FIGURE 9 Fraction of a'- and c-axis oriented crystallites as a function of take-up stress. From Spruiell and White.¹⁵ (With permission of John Wiley and Sons, New York.)

spin stress has been evaluated¹⁵ and is shown in Figure 9. The effect of quench rate¹³ on the resulting "as spun" morphology has been confirmed; a highly oriented smectic structure showing only c-axis orientation is obtained by water quench, while a monoclinic crystalline fiber with both c and a'-axis

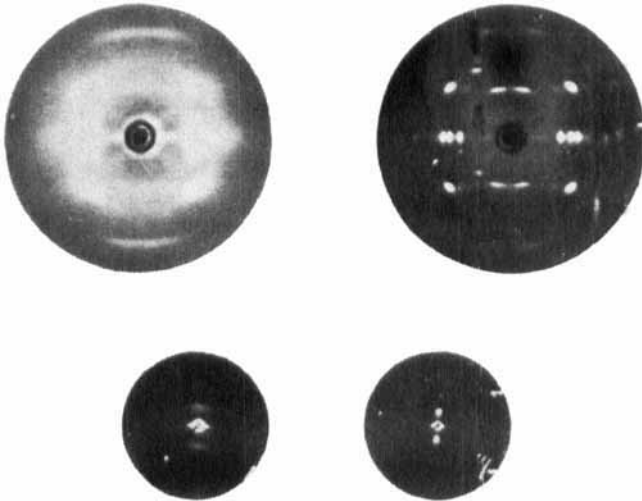


FIGURE 10 WAXR (top) and SAXR (bottom) diffraction patterns of spin oriented smectic (left) and crystalline (right) polypropylene.

orientation forms with air cooling. In addition, SAXR indicates a fibrillar structure for the smectic and a typical lamellar structure for the crystalline material (Figure 10). This proves the earlier proposed mechanism: stress induced fibrillar nuclei, followed by fibril formation, and eventually lamellar epitaxial over-growth and formation of both the c and a' -axis oriented systems. The water quench stops this process prior to the onset of epitaxial over-growth.

PET spin orientation work was first published by Liska.¹⁷ (Extrusion conditions: Temp.: 292°C, diameter of spinnerette hole: 0.4 mm. Spinning to constant denier and number of filaments: (112/20). Take-up speeds: 1,450–4,000 m/min, polymer viscosity $\eta_{\text{spec}} = 0.74$ and 0.88.) Again the effect of molecular weight and spinning speed determine the “as spun” structure. Figures 11 and 12 show the effect of increasing spinning speed (at constant final denier) for two samples of different molecular weight. The high molecular weight material (Figure 12) at high speed is well-oriented and crystalline, the small angle pattern indicating the presence of fibrillar voids. The more detailed study of the low molecular weight material (Figure 11) shows an amorphous material gradually developing some crystallinity and good orientation. Annealing of this series reveals a peculiar change from a to c axis orientation with increasing spinning speed. This may be due to the same transition from spherulitic to lamellar morphology as originally proposed by Keller *et al.*¹⁸ and shown above in the case of PE¹¹ and PP.^{10,14} The SAXR patterns are not conclusive with respect to the “as spun” structure, since the major part of the observed

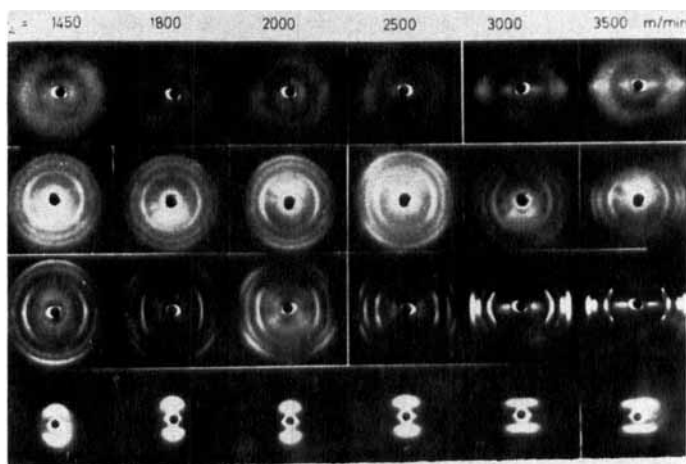


FIGURE 11 WAXR and SAXR patterns of PET yarns of increasing spinning speed (V_A); $[\eta] = 0.74$. Row 1, WAXR of yarns “as spun”; Rows 2 and 3, WAXR of these samples after annealing, free to shrink or at constant length (C.L.), respectively; Row 4, SAXR of annealed samples (C.L.). From Liska.¹⁷ (With permission of Dr. Dietrich Steinkopff Verlag, Darmstadt.)

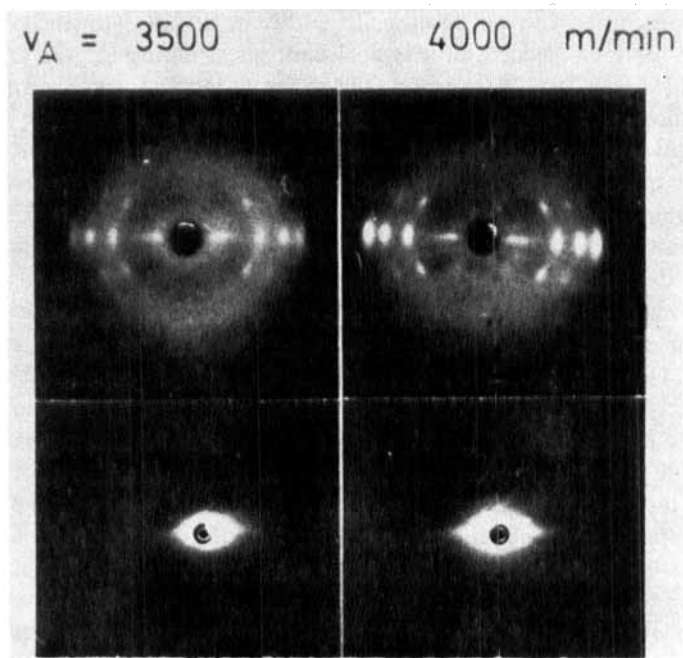


FIGURE 12 WAXR (top) and SAXR (bottom) of as spun PET at high spin speeds (V_A); $[\eta] = 0.88$. Fibers "as spun". From Liska.¹⁷ (With permission of Dr. Dietrich Steinkopff Verlag, Darmstadt.)

crystalline structure probably forms in the annealing step. However, also here, the SAXR (at the highest speed; 3,500 m/min) indicates a fibrillar rather than a lamellar morphology in spite of relaxation during annealing. Since the PET crystallization rate is very slow, epitaxial over-growth to form lamellae as in polypropylene cannot take place prior to immobilization of the fiber structure. At the Fiber Society meeting in Asheville, Huisman and Heuvel¹⁹ presented an excellent study of PET high speed spinning, evaluating the resulting structures via thermal and thermomechanical analysis, birefringence, and X-ray diffraction. (Extrusion conditions: Temp.: 290°C, capillary diameter: 0.25 mm. Spinning to constant denier and number of filaments (150/30). Take-up speeds: 2,000–6,000 m/min. Melt flow rate per single spinnerette orifice variable from 1.11 g/min at 2,000 m/min to 3.34 g/min at 6,000 m/min take-up speed. $\eta_{spec} = 0.63$ (1 g PET/100 g metacresol at 25°C).) Figure 13 shows the effect of increased take-up speed and stress on crystallinity and orientation. Crystallinity increases, and the orientation of the crystallites is excellent as soon as they form. Differential thermal analysis curves of these fibers as a function of spin stress show a decreasing crystallization exotherm as spinning speed increases.

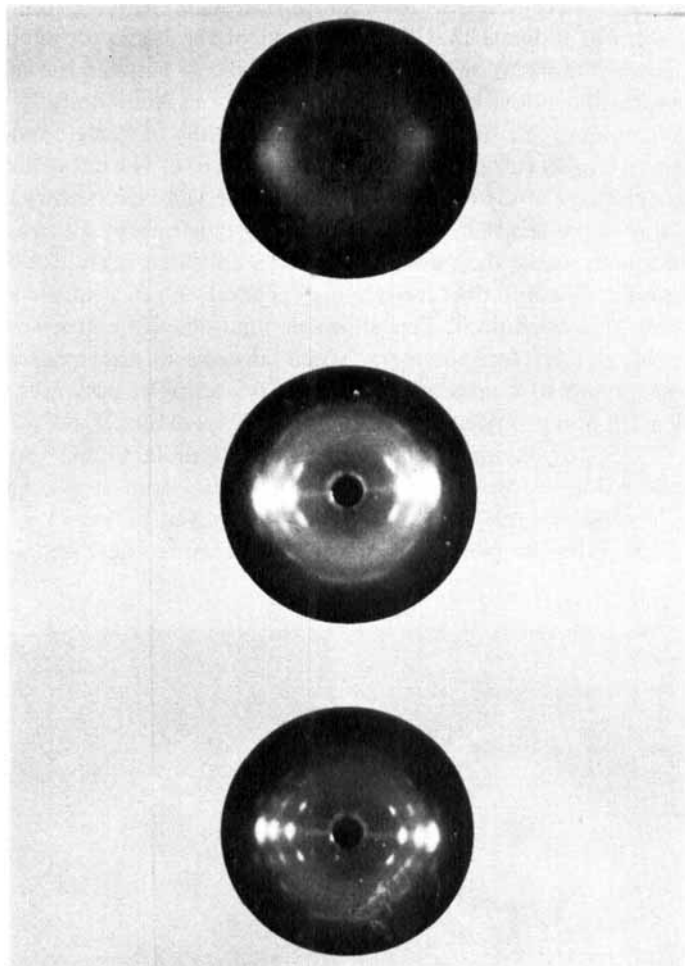


FIGURE 13 WAXR patterns of PET as a function of take-up velocity (top-to-bottom: 4,000, 5,000, 6,000 m/min).

In addition, the temperature of crystallization decreases in the same direction, indicating that the increased orientation in the amorphous regions or the presence of oriented crystallites allows crystallization at a lower temperature.

Thus, in principle, both polypropylene and PET show the same stress crystallization mechanism. Fibrillar nuclei form extended chain fibrillar crystal structures which, if the rate of crystallization under operating conditions is faster than the quench rate, may lead to epitaxial over-growth and formation of the typical lamellar morphology.^{14,20}

The above data of crystallization under spin stress and with high temperature gradients seem to indicate that the formation of the highly developed, well oriented lamellar morphology is an intermediate stage between the spherulitic superstructure under low stress extrusion conditions and the fully oriented fibrillar morphology possibly obtainable under really extreme conditions of spin stress and temperature gradients along the spin line. The initial discovery²⁰ of this morphology and of the hard elastic materials (see below) is a consequence only of the fact that for some specific polymers in melt extrusion processes under high stress, the tremendous increase in their crystallization rates makes crystallization and fiber morphology generation rates equal to or faster than the melt spin operations. This allows enough time for extensive epitaxial lamellar over-growth for polymers which already in the quiescent state crystallize fast and to a large extent. Thus, for example, polymers such as: polyethylene,¹⁵ polypropylene,^{14,21} poly(4-methylpentene),¹⁴ poly(3-methylbutene),^{14,21-22} polyoxymethylene,^{21,23,14} poly(pivalolactone),²⁴ and poly-(isobutylene oxide),²⁵ on extrusion under adequate spin stress, have been shown to develop the lamellar superstructure. However, polymers with slower crystallization rates, in principle, should also acquire the mechanical and

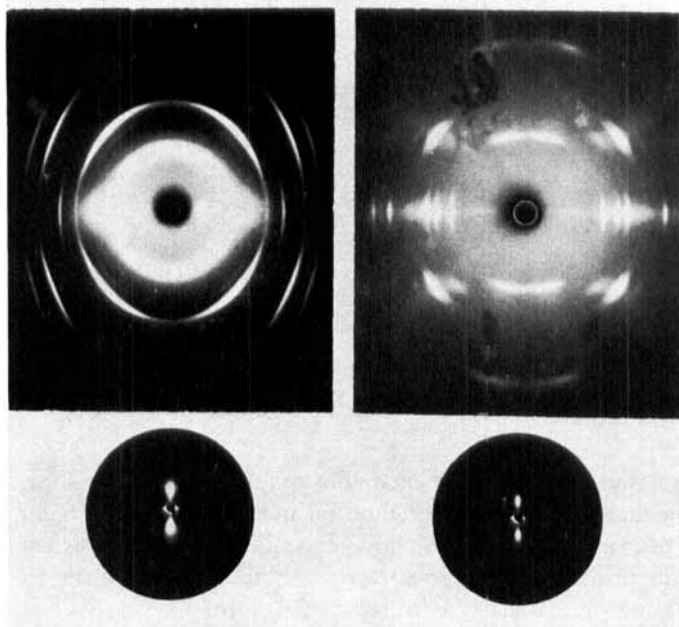


FIGURE 14 WAXR (top) and SAXR (bottom) patterns of "as spun" Celcon® (left) and polypropylene (right). From Noether and Whitney.¹⁴ (With permission of Dr. Dietrich Steinkopff Verlag, Darmstadt.)

thermal characteristics of these materials provided they are converted to the oriented, lamellar morphology.²⁶

The major feature of good, hard elastic materials is a highly crystalline, well oriented, lamellar superstructure with lamellae of uniform thickness, large lateral extent, and relatively few load-bearing interlamellar links, obtained by annealing a spin-stress oriented film or fiber at 20–40°C below the polymer melting point.¹⁴ The name “hard” elastic was coined, since fibers of this kind showed extremely high elastic recoveries from 50–100% extension, similar to rubber; however their initial modulus is considerably higher, i.e. between 10–40 g/den.

The “as spun” hard elastic materials show good orientation and a typical, fan-like SAXR pattern (Figure 14). With increasing annealing temperature

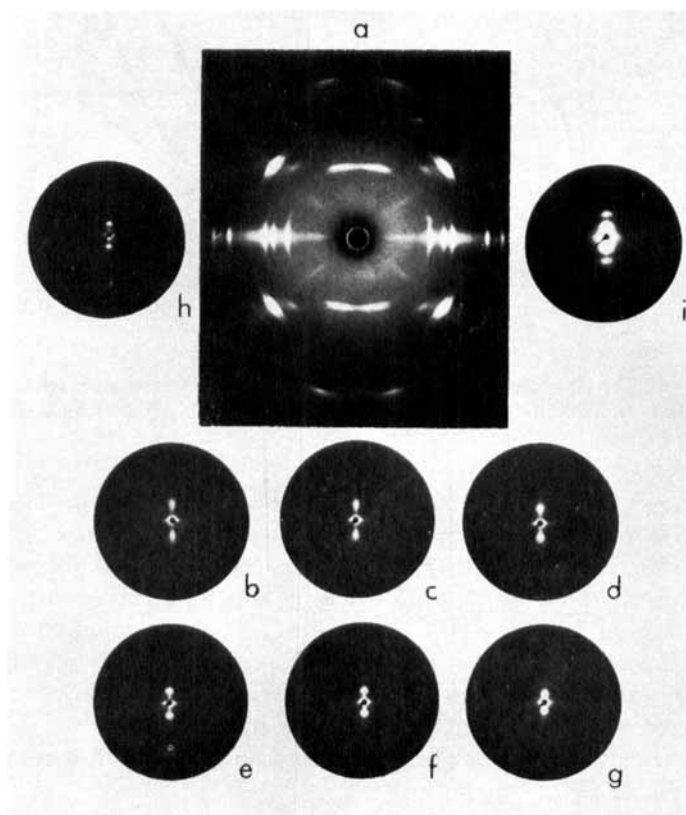


FIGURE 15 WAXR and SAXR of polypropylene as a function of annealing temperature. (a), WAXR (150°C/1 hr). SAXR data: (b) 70°C/1 hr; (c) 90°C/1 hr; (d) 120°C/1 hr; (e) 140°C/1 hr; (f) 155°C/1 hr; (g) 160°C/1 hr; (h) 150°C/1 hr, SAXS exposure $\frac{1}{4}$ hr; (i) 150°C/1 hr, SAXS exposure 16 hr. After Noether and Whitney.¹⁴

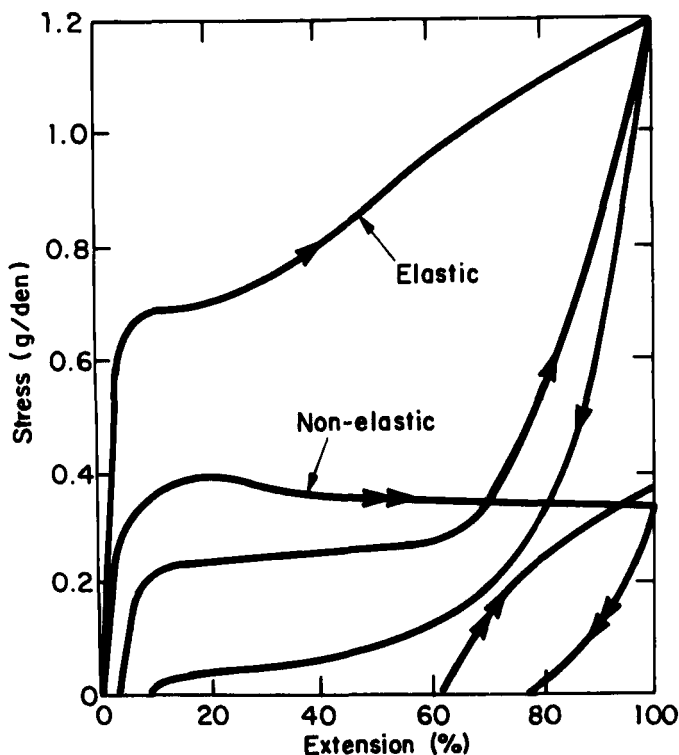


FIGURE 16 Tensile curves of polypropylene fibers at room temperature (elongation rate 100%/min). From Park and Noether.²⁷ (With permission of Dr. Dietrich Steinkopff Verlag, Darmstadt.)

this fan gradually turns into sharp spots, the uniformity of the long spacing being perfect enough to allow the appearance of the second order spacing (Figure 15i). The tensile curve at room temperature shows up to 97–98% immediate recovery from 50–100% extension (Figure 16) and even at very low temperatures (–150 to –180°C), the elastic recovery is about 50% with the fiber having an elongation at break of 80%, compared to 3–5% for normal fibrillar or rubbery materials (Figure 17). While the modulus of the fibers gradually decreases with increasing temperature²⁷ (Figure 18), the elastic recovery remains high even close to the annealing temperature (for example, 145°C) (Figure 19).

X-ray diffraction, electron microscopy, light scattering, and density measurements show that the elastic characteristics are based on the development of voids between the lamellae; the void size in the extrusion direction being proportional to the degree of extension.¹⁴ WAXR shows only slight changes

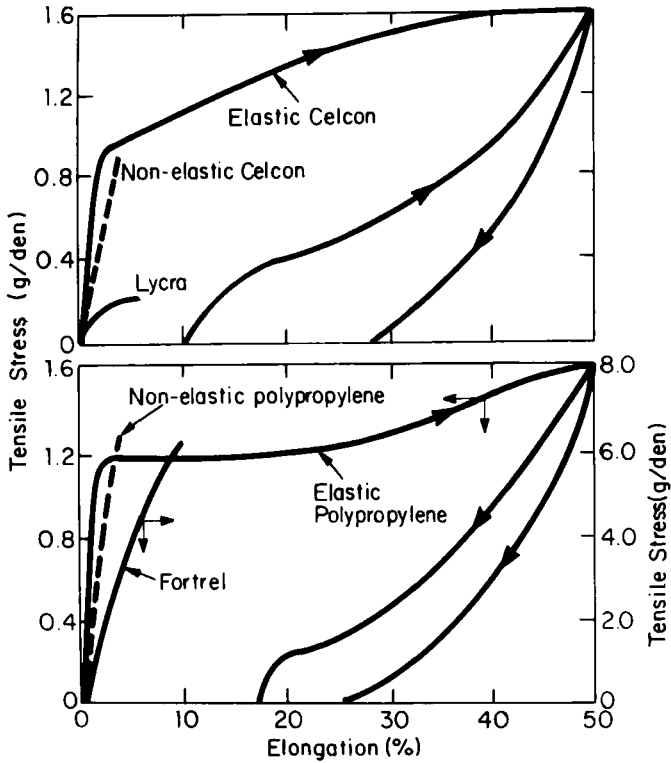


FIGURE 17 Tensile curves of Celcon®, polypropylene, polyester (Fortrel®), and spandex (Lycra®) fibers at -190°C (elongation rate 100%/min). From Park and Noether.²⁷ (With permission of Dr. Dietrich Steinkopff Verlag, Darmstadt.)

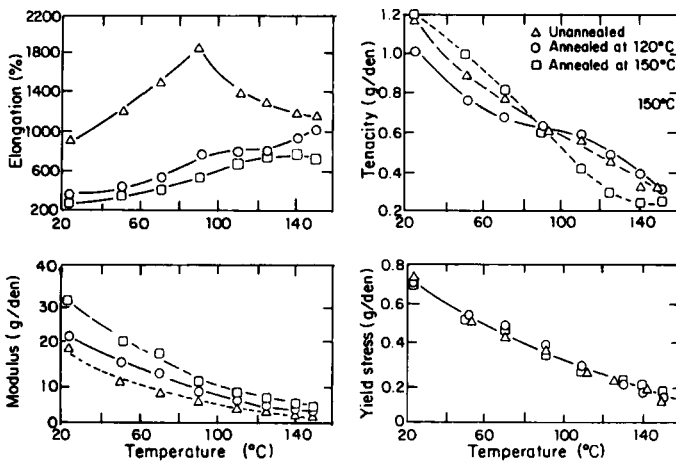


FIGURE 18 Temperature dependence of tensile properties of elastic polypropylene fibers (elongation rate 100%/min). From Park and Noether.²⁷ (With permission of Dr. Dietrich Steinkopff Verlag, Darmstadt.)

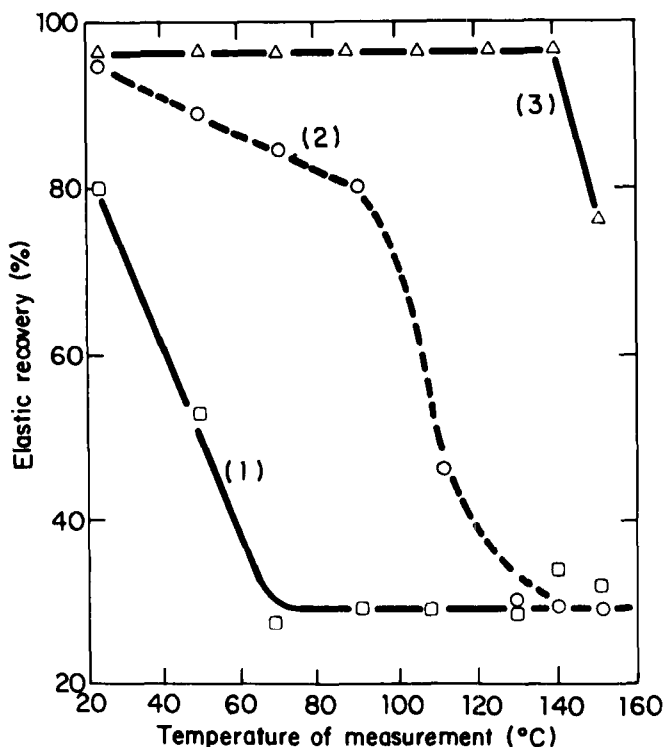


FIGURE 19 Temperature dependence of elastic recovery of elastic polypropylene fibers: (1) "as spun"; (2) annealed at 120°C; (3) annealed at 150°C (extension rate 100%/min to 100% extension). From Park and Noether.²⁷ (With permission of Dr. Dietrich Steinkopff Verlag, Darmstadt.)

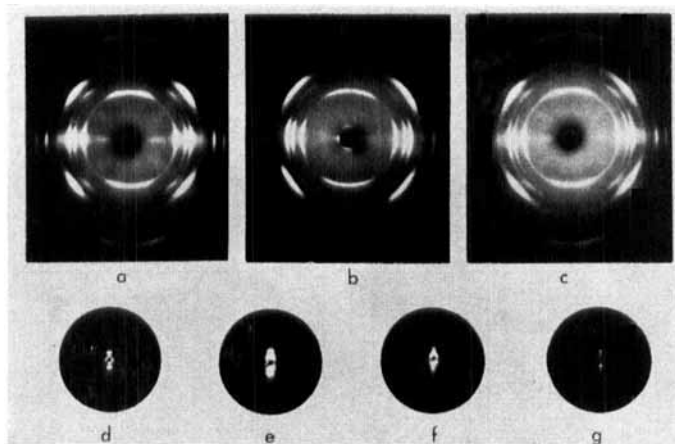


FIGURE 20 WAXR patterns of polypropylene on extension to 73% and relaxation (from left-to-right: 0% extension, 73% extension, back to 0% extension). SAXR patterns (from left-to-right): 0%, 50%, 100%, and back to 0% extension. From Noether and Whitney.¹⁴ (With permission of Dr. Dietrich Steinkopff Verlag, Darmstadt.)

in orientation, SAXR shows a tremendous increase in scattering intensity (Figure 20) though on relaxation to zero stress, the original SAXR and WAXR pattern prior to extension are recovered. The same is apparent from electron microscopic data (Figure 21). In "as spun" materials the recovery is not

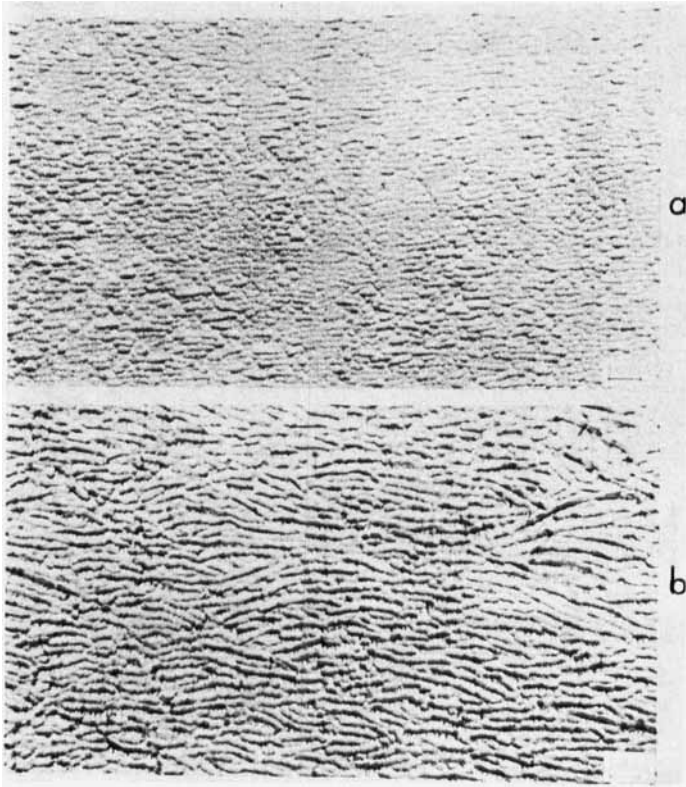


FIGURE 21 Electronmicrograph of polypropylene annealed at 144°C. (a) 0% extension, (b) 80% extension. Direction of stretch: vertical. After Noether and Whitney.¹⁴

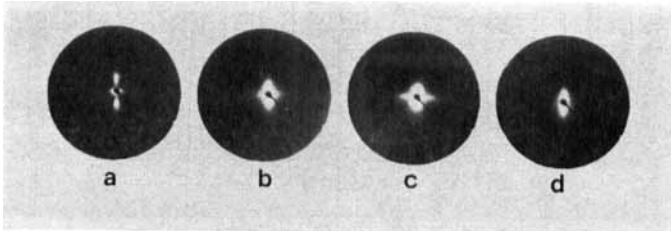


FIGURE 22 SAXR pattern of "as spun" polypropylene as a function of extension: (a) 0%; (b) 30%; (c) 100%; (d) back to zero stress after extension. Fiber direction: vertical. From Noether and Brody.²⁸ (With permission of Textile Research Institute, Princeton.)

complete. Some irreversible deformation has occurred which is visible in residual void scattering in the relaxed structure (Figure 22).^{14,28} The recovery process shows immediate extensional recovery from stretch; however, regeneration of the original stress-strain curve extends to a few hours^{27,29} or days depending on the temperature at which the relaxed yarn recovers (Figure 23).

The original model proposed for the extension recovery mechanism was that of a set of lamellar leaf springs, interconnected in the interlamellar surfaces by unknown links (fibrils, loops, crystal connectors, Figure 24). A slightly more sophisticated model introduced the reduction of the surface energy on relaxation as the driving force, tending to close the voids.^{14,30} The original leaf spring model did not allow for entropy effects; however, Göritz and Müller³⁰ showed by simultaneous thermal and mechanical measurements that the hard elastic

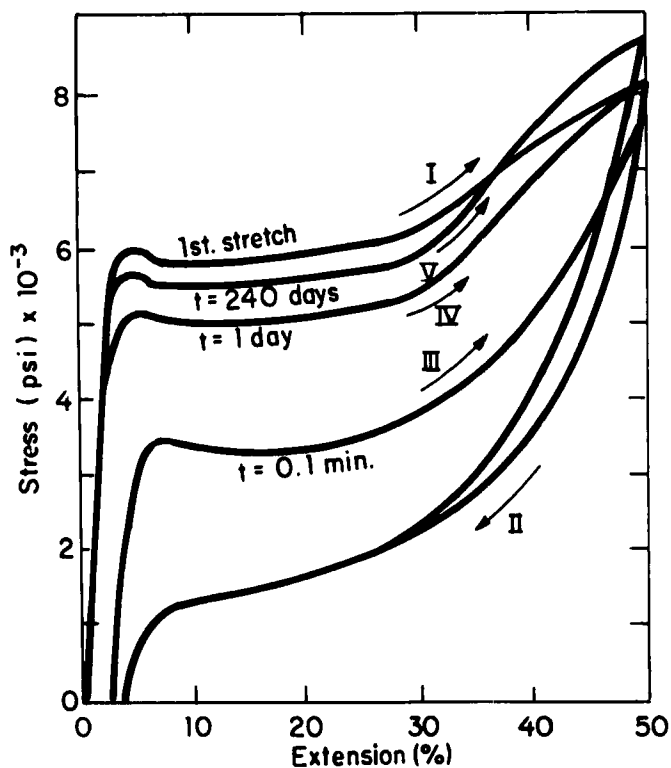


FIGURE 23 Stress-strain recovery behavior of elastic polypropylene film as a function of time interval between first and second extension cycle. I, first extension curve; II, first recovery cycle. Second extension curve: III, after 0.1 min; IV, after one day; V, after 240 days. From Park and Noether.²⁷ (With permission of Dr. Dietrich Steinkopff Verlag, Darmstadt.)

materials had an intermediate position between steel and rubber, the former being completely energy elastic, the latter entropy elastic, while these fibers had both energy and entropy elastic components (Figures 25 and 26).

Considerably more work is required to elucidate the real extension mechanism; the type and concentration of tie points and the reasons for the differences in the rates of recovery of extension and modulus.²⁷ For the same morphology, polyethylene, polypropylene, etc., show vastly different elastic recoveries, a feature probably related to details of interchain cohesive strength and crystal packing of each polymer.

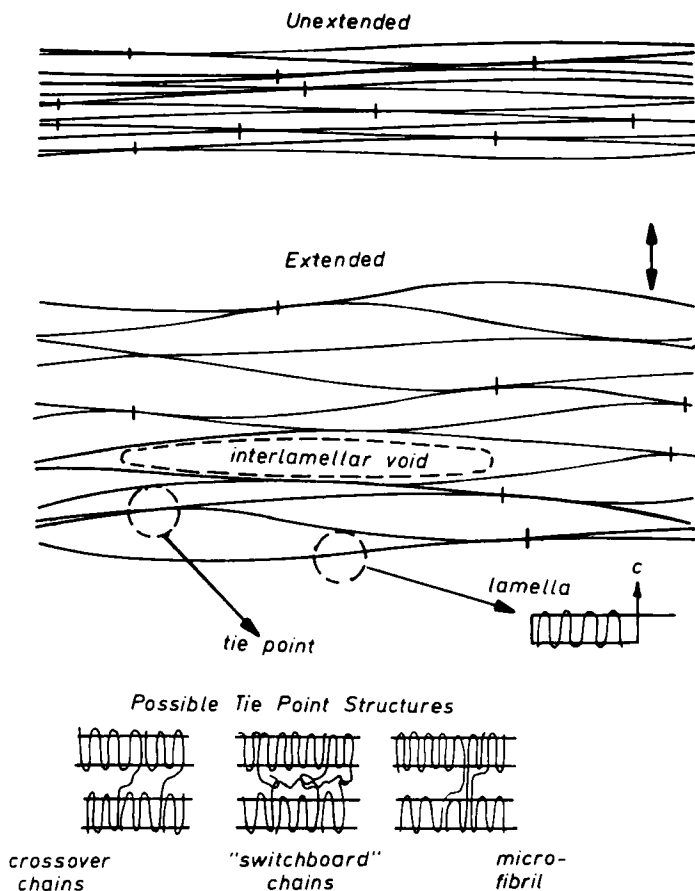


FIGURE 24 Simple lamellar model "Leaf Spring". From Noether and Whitney.¹⁴ (With permission of Dr. Dietrich Steinkopff Verlag, Darmstadt.)

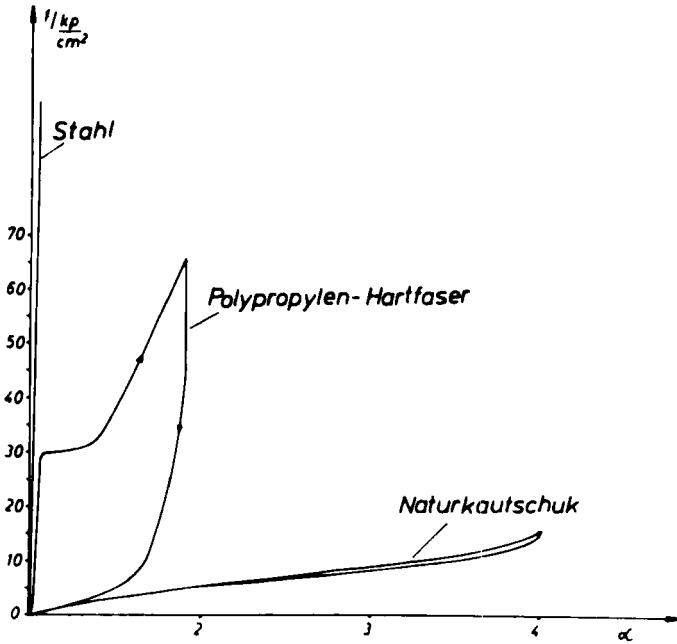


FIGURE 25 Stress-strain curves for steel, rubber, and hard elastic fibers. From Göritz and Müller.³⁰ (With permission of Dr. Dietrich Steinkopff Verlag, Darmstadt.)

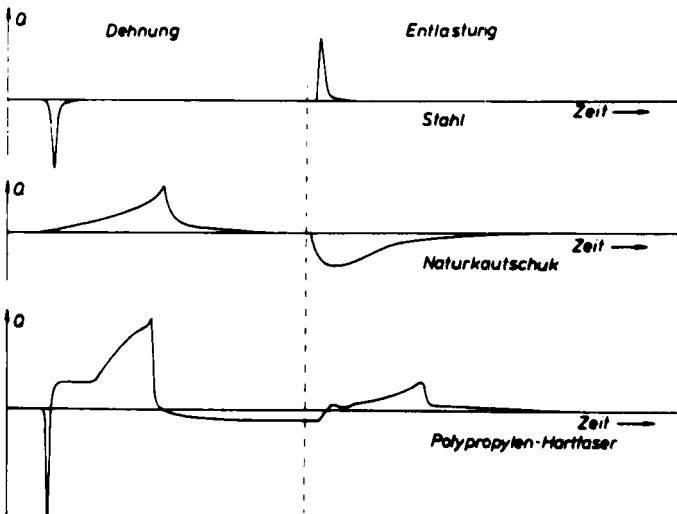


FIGURE 26 Curves of heat flow for extension and relaxation of steel, rubber, and hard elastic fibers. From Göritz and Müller.³⁰ (With permission of Dr. Dietrich Steinkopff Verlag, Darmstadt.)

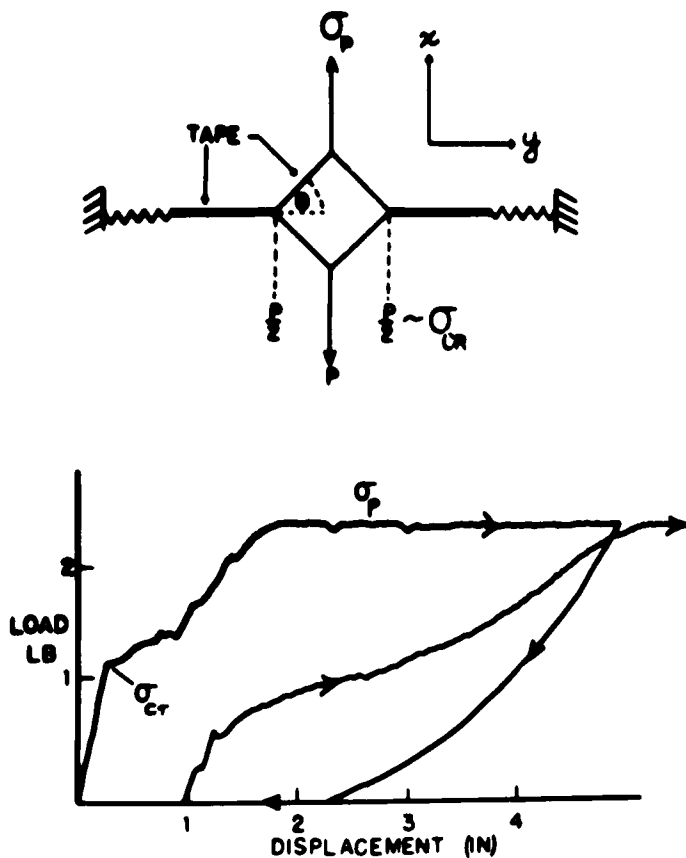


FIGURE 27 Adhesive tape test (top) and tensile behavior (bottom). After Wool.³¹ (With permission of John Wiley and Sons, New York.)

Wool³¹ has recently shown that a mechanical model consisting of two layers of paper tape and two springs, on extension normal to the surfaces, shows exactly the same elastic behavior as the hard elastic fibers (Figure 27).

There are at present no industrial applications making use of the tensile characteristics of the "as spun" or annealed hard elastic materials. However, the extensive formation of fully accessible microvoids on extension has led to the development of the microporous material "Celgard[®]" with a fully stabilized void structure (Figure 28). This material finds use in medical applications and as membranes.

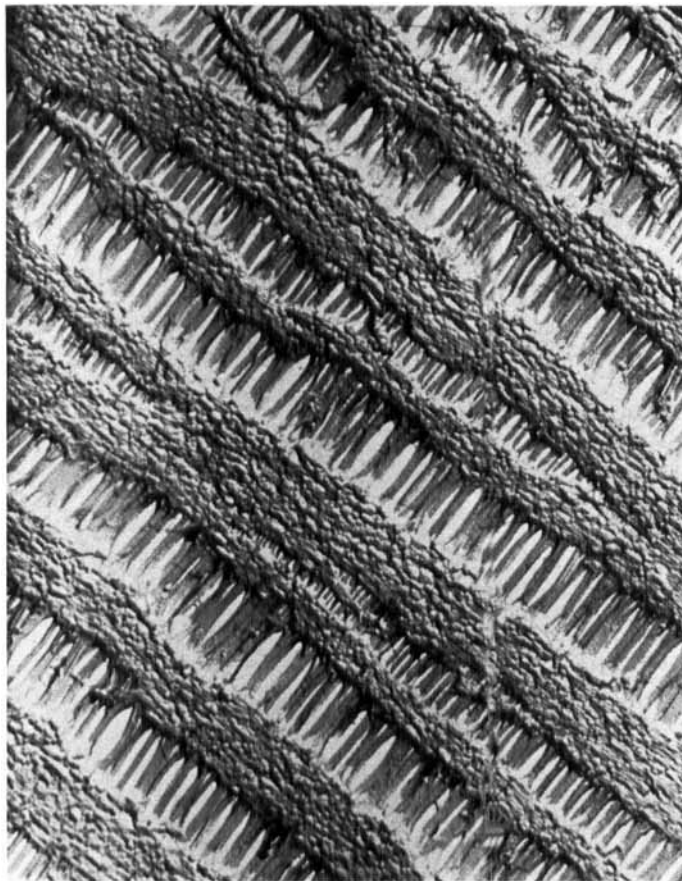


FIGURE 28 Electronmicrograph of Celgard® microporous material. The thickness of the lamellae in the unextended parts of the material is about 180–200 Å. (Photo courtesy of Dr. I. Hay.)

SUMMARY

The study of crystallization in processes involving high temperature and pressure gradients up to the present has been concerned primarily with melt-spinning and therefore with processes involving temperature gradients.

Experimental data and theories for a few of these systems such as nylons, polyesters, polyethylene, and polypropylene have been published. Primarily the structural, morphological, thermal, and mechanical characteristics of the products have been analyzed as function of extrusion conditions (temperature,

spin-stress, quench rate). Direct observations of the spin-line, due to experimental difficulties, so far have been limited to observations of monofilaments of rather heavy denier.

The stress-spin orientation studies have led to materials with a special morphology and mechanical characteristics: hard elastic fibers and films. These have a highly crystalline, very uniform, oriented lamellar morphology. Their elastic characteristics (90–98% recovery from 50–100% extension) as elucidated by X-ray diffraction, electron microscopy, light scattering, pore size analysis, etc., indicate a reversible extension-deformation process involving void formation. The simplest leaf-spring type model proposes the rupture of the interlamellar regions which open into voids and close again on relaxation of stress. The mechanism seems largely energy controlled.

The well-oriented, lamellar structure, obtained by stress spin-orientation and perfected by subsequent annealing, appears to be of an intermediate morphology between the spherulitic structure obtained at slow spinning rates and low stresses and a preferentially fibrillar structure achievable at extreme temperature gradients and spin stresses for polymers with fast crystallization rates. Slow crystallizers, such as PET, yield crystalline, fibrillar morphologies during stress spinning at high take-up speeds. Here the fiber formation process prior to solidification does not provide adequate time for epitaxial over-growth and, therefore, extensive formation of lamellar morphologies does not occur.

References

1. J. L. White (Ed.), Fiber and yarn processing, *Appl. Polymer Symp.* **27** (1975); (see especially papers on pages 1, 61, 111, 121). Also Ref. 8.
2. K. Katayama, T. Amano, and K. Nakamura, *Kolloid Z.Z. Polymere* **226**, 125 (1968).
3. A. Ziabicki, *Fundamentals of Fibre Formation* (John Wiley and Sons, New York, 1976).
4. J. W. S. Hearle and R. H. Peters, *Fibre Structure* (The Textile Inst. Butterworths, 1963).
5. H. Blades and J. R. White, U.S. 3,081,519 (3/19/63) to Du Pont.
5. W. H. Bonner and M. Q. Webb, Textile Dept., Du Pont. Fiber Society meeting, April 28–30, 1976, Montreal, Canada.
6. For example: W. Griehl and H. Versäumer, *Faserforsch. u. Textiltech.* **9**, 226 (1958).
7. ACS Symposium on Stress Induced Crystallization. J. H. Southern (Ed.), *Polym. Eng. & Science* **16** (3) 126–222 (1976), *Polymer Preprints* **16** No. 2 (1975).
8. J. R. Collier, T. Y. T. Tam, J. Newcome, and N. Dinos, *Polym. Eng. & Science* **16**, 204 (1976).
9. A. Peterlin, *Polym. Eng. and Science* **16**, 126 (1976).
10. J. E. Spruiell and J. L. White, *Polym. Eng. and Science* **15**, 660 (1975).
11. J. R. Dees and J. E. Spruiell, *J. Appl. Poly. Sci.* **18**, 1053 (1974).
12. B. Wunderlich, *Macromol. Physics*, Vol. II (Academic Press, New York, 1976), p. 77.
13. W. C. Sheehan and T. B. Cole, *J. Appl. Poly. Sci.* **8**, 2359 (1964).
14. H. D. Noether and W. Whitney, *Kolloid Z.Z. Polymere* **251**, 991 (1973); B. S. Sprague, *J. Macromol. Sci.-Phys.* **B8**, (1–2) 157 (1973).
15. J. E. Spruiell and J. L. White, *Appl. Polym. Symposia* **27**, 121 (1975).
16. E. S. Clark and J. E. Spruiell, *Polym. Eng. and Science* **16**, 176 (1976); P. V. F. Fung, E. Orlando and S. H. Carr, *Polym. Eng. Sci.* **13**, 295 (1973); F. Khoury, *J. Res. Natl. Bur. Stds.* **70A**, 29 (1966).

- 16a. D. Göritz and F. H. Müller, *Coll. Polymer Sci.* **252**, 862 (1974).
17. E. Liska, *Kolloid Z.Z. Polymere* **251**, 1028 (1973).
18. A. Keller and M. J. Machin, *J. Macromol. Sci.* **B1**, 41 (1967).
19. H. M. Heuvel and R. Huisman, Fiber Society Conference, Asheville, N.C., May 18–20, 1977. Preprint, to be published in *J. Appl. Poly. Sci.*
20. S. L. Cannon, G. B. McKenna, and W. O. Statton, *J. Polym. Sci., Macromol. Reviews* **11**, 209 (1976).
21. R. G. Quynn and H. Brody, *J. Macromol. Sci.* **B5**, 721 (1971); R. G. Quynn, H. Brody, S. E. Sobering, I. K. Park, R. L. Foley, H. D. Noether, W. Whitney, R. Pritchard, M. A. Sieminski, J. D. Hutchinson, H. L. Wagner, K. Sakuoku, and R. Corneliussen *J. Macromol. Sci.* **B4**, 953 (1970).
22. R. G. Quynn and B. S. Sprague, *J. Poly. Sci., Pt. A2*, **8**, 1971 (1970).
23. C. A. Garber and E. S. Clark, *J. Macromol. Sci.* **B4**, 499 (1970).
24. F. W. Knobloch and W. O. Statton, USP 3,299,171 (1/17/67) to Du Pont.
25. T. Yamazaki, S. Oya, N. Tsukane, K. Tanaka, H. Toba, and K. Yamagishi, *Polymer* **16**, 425 (1975).
26. H. D. Noether, USP 3,513,110 (5/19/70) to Celanese.
27. I. K. Park and H. D. Noether, *Coll. Polym. Science* **253**, 824 (1975).
28. H. D. Noether and H. Brody, *Text. Res. J.* **46**, 467 (1976).
29. D. Göritz, Private communication (1977).
30. D. Göritz and F. H. Müller, *Coll. Polym. Science* **253**, 844 (1975).
31. R. P. Wool, *J. Poly. Sci., Polym. Phys. Ed.* **14**, 603 (1976).